Optimizing the Anticancer Effect of Doxil Using Pharmacokinetic and Pharmacodynamic Modelling

Cherong Ma [1,*], Zekai Guo [1], Zhiyin Liang [1], and Virgia Wang [2]

[1] Shenzhen College of International Education, Shenzhen, China; Email: s20217.guo@stu.scie.com.cn (Z.G.), 1370331613@qq.com (Z.L.)

[2] Shanghai Jiao Tong University, Shanghai, China; Email: virgiathekite@gmail.com (V.W.)

*Correspondence: macherongring@outlook.com (C.M.)

***Abstract*—Liposomal Dox, Doxil, enhances the antitumor effect of Doxorubicin by increasing its delivery ability to tumors. Therefore, quantitative studies on the relationship between the antitumor effect and liposomal characteristics will help to optimize the clinical application of Doxil in cancer treatment. Herein, we develop a physiological model to compute the pharmacokinetics and pharmacodynamics of Doxil, to calculate the time course of free Dox in the tumor space and linked this with a cell-killing kinetic model to quantify its anticancer effect. In this research, the two models utilize parametric figures of drug transportation in anatomical compartments, including plasma, capillary, interstitial, and tumor cells, to simulate the relationships between intravenously injected Dox and Doxil. Furthermore, simulations are performed to discuss the relationship between the anticancer effect and physicochemical properties, by comparing pharmacological parameters of Doxil.**

***Keywords*—Dox (Doxorubicin), liposome, cancer treatment, chemotherapy, drug delivery system, pharmacokinetics, pharmacodynamics, antitumor effect, computational modelling, simulation, physical alternation, proliferation rate, clearance rate**

I. Introduction

Doxorubicin (Dox), an anthracycline, is a commonly used anticancer drug in a variety of cancer types including breast cancer, ovarian cancer, and lung cancer [1]. Dox kills cancer cells by inhibiting the activity of topoisomerase II and intercalating into DNA and stopping replication and transcription. However, clinical applications of dox are limited by its cardiotoxicity [2], which can lead to cardiomyopathy and congestive heart failure [3]. Moreover, the utilization of Dox suffers from a high rate of clearance, which shortens circulation lifetime and limits drug exposure [4].

These challenges have inspired the invention of the nanoparticle-based delivery system, including polypeptide micelles, gold nanoparticles, and liposomes (a bilayer vesicle assembled from amphiphilic phospholipids) [5]. Among those delivery systems, only Doxil, a liposomal formulation of Dox, received the approval of the Federal Drug Administration [6].

The lipid bilayer can protect inner Dox from premature release, prolonging its circulation time, increasing overall drug exposure, and avoiding systemic toxicity. Moreover, the drug can selectively accumulate in the tumoral area via Enhanced Permeability and Retention (EPR) effects (resulting from porous tumor vasculature) [7]. In short, Doxil has improved pharmacokinetics and targeted accumulation compared with free Dox.

Due to the apparent advantages of Doxil over Dox, the use of Doxil is becoming the predominant chemotherapy in cancer treatment. So far, although the efficacy and toxicity of Doxil has been investigated for years, the delivery parameters of Doxil are not completely optimized to achieve the best efficacy while sparing systemic toxicity. The pharmacokinetics parameters of liposomal Doxil not only affect the delivery efficiency of Dox but also determines the antitumor efficacy. Hence studying the delivery parameters of Doxil helps us to optimize its use. Previous studies have also cited and supported this action because it benefits the field's overall understanding of drug metabolism [8]. Pharmacokinetics (PK) and Pharmacodynamics (PD) essentially describe the relationship between drug potency, drug concentration, and time. Thus, PK and PD-based mathematic models are often constructed to study the use of a specific drug in different clinical settings.

Herein, we established mathematical models to evaluate the delivery parameters of Doxil from the perspective of PK and PD. Our model allows for quantitative evaluation of drug delivery systems and helps to optimize the drug delivery strategies of cytotoxic agents. We designed the models with different aims: (i) quantitatively investigating the influence of Doxil parameters on antitumor efficacy; (ii) analyzing the effect of physiological alterations on Doxil potency; (iii) understanding how tumor sensitivity and invasiveness affect Doxil efficacy.

This work is significant in multiple ways. Primarily, developing mathematical PK models optimizes the

Manuscript received March 8, 2023; revised May 15, 2023; accepted May 25, 2023.

modification of liposome parameters, thereby increasing tumor drug exposure while saving normal tissues. Moreover, it will be feasible to predict cell-level toxicity by precisely manipulating the parameters of liposomes, thus enabling the prediction of cytotoxicity.

II. Methods

A multi-compartment PK and PD model was established to simulate the delivery system of Dox and Doxil. Considering the intrinsic complexity of the human body, we simplified the whole organism by categorizing the whole body into four major compartments: plasma, reticuloendothelial system, normal tissue, and tumor. Plasma represents the systemic circulation system by which Doxil is transported throughout the body. The reticuloendothelial system is another major system that is responsible for Doxil clearance. Normal tissue and tumoral tissue deposition of Doxil are separately considered to distinguish the effect of Doxil in two types of cells. In order to investigate the detailed distribution within the tumor and understand the performance of Doxil on a cell scale, the tumor sub-compartment was then divided into three parts: tumoral capillary, interstitial space, and tumor cell. The interrelated mathematical connections between them helped us to develop formulas and establish the model.

Doxil is intravenously administered into the systemic circulation, so within the plasma, the Doxil is transported to major organs and tissues by the bloodstream. Another destination of Doxil is the Reticuloendothelial System (RES), which significantly filters Doxil out from circulation, resulting in degradation. RES consists of reticular connective tissue and multiple types of phagocytes. On the one hand, reticular connective tissues made from collagen and stoma-like labyrinth can trap Doxil by their stretched stoma-like protein structure. On the other hand, the phagocytic cells in the RES, such as Kupffer cells and macrophages, can eliminate Doxil by phagocytosis. However, the Polyethylene Glycol (PEG) coat on the Doxil enables the abscondence from opsonization and immediate recognition initiated by cells in RES [9]. Additionally, it impedes the protein corona formation and enhances the steric endurance of liposomal layers to guarantee extrication only at the targeted organ.

In the subsequent locomotion, Doxil is carried by the bloodstream from the capillary to the tumor via an interstitial space. The capillaries at the site of the tumor are morphologically atypical. The loosely contacted leaky gaps on the capillary walls are excavated initially for nutrient requirements of tumor cells. Nevertheless, the structure provides higher feasibility for the extravasation of Doxil from intravascular space to the tumor. In a tumor with a relatively acidic environment (PH level 4~5) in comparison to the normal tissue (PH level around 7), due to the effect of anaerobic respiration, the Doxil's activities will be favored by the Warburg effect (a reference to details contributed by 'national center for biotechnology information') [8, 10] because of the absence of most of the immune cells, and release at a higher rate. From further micro-prospect, according to the review of the liberating mechanism of liposomal medicine [11], the endosome will combine with the lysosomes resulting in the production of secondary lysosomes, and the liposome will be sundered by enzymes. Meanwhile, the important trait (number of cations surrounded) of liposome is changed [12], leading to intranuclear destabilization, therefore the emancipation of drugs.

In the case of Dox, there is a high similarity between their journeys. In fact, as the release of Doxil in tumors is proven to be relatively less effective in comparison with the one of Dox [11, 13], Dox is the primary source of drugs for the tumor. By accessing the pathways of Doxil and Dox, models were established.

A. PK Model

The model aims to simulate the change in concentration of drugs when Doxil is intravenously injected into our bodies. As we discussed (Fig. 1B), four compartments are involved in our model: RES, normal tissue, plasma, and tumor. The tumor is further distributed into capillary, interstitial fluid, and tumor cells. The green circles in the graph represent the Doxil in that compartment, whereas the white square represents the concentration of free Doxorubicin in that area. The circulation of Free Dox and Doxil is summarized into eight mass equations.

Doxil in plasma:

$$V_p \times \frac{dC_{p\,lipo}}{dt} = Q \times C_{p\,lipo} - K_{re} \times V_{p\,lipo} \times C_{p\,lipo} - K_{res} \times V_p \times C_{p\,lipo} - Q \times C_{p\,lipo} \quad (1)$$

Doxil is first administered into the plasma, and Doxil in the plasma circulates throughout the body with four major destinations: (i) Doxil is phagocyted and removed by RES, which has the rate constant K_{res}. Therefore, the rate of mass decrease of Doxil can be calculated by rate×concentration, which gives $-K_{res} \times C_p \times V_p$; (ii) blood flows into the tumoral capillary represent another mass decrease, governed by the blood flow rate Q. The rate of decrease is the concentration of Doxil×flow rate, or $-Q^* C_{p\,lipo}$; (iii) Doxil in plasma releases payload into the plasma at a rate of K_{re}, due to membrane instability, which gives $-K_{re} \times C_p \times C_p$; (iv) Doxil in the capillary also flow back to plasma at the rate of Q, contributing to an increase equal to $C_{cap\,lipo} \times Q$. All monomials add up to a whole equation that concludes the rate equation of Doxil in plasma. The parameters are shown in Tables I and II.

Doxil in capillary:

$$V_{cap} \times \frac{dC_{cap\,lipo}}{dt} = Q \times C_{p\,lipo} - K_{tu} \times V_{cap} \times C_{cap\,lipo} - K_{re} \times V_{cap} \times C_{cap\,lipo} - Q \times C_{cap\,lipo} \quad (2)$$

Doxil in interstitial space:

$$V_{int} \times \frac{dC_{int\,lipo}}{dt} = K_{tu} \times V_{cap} \times C_{cap\,lipo} - K_{re} \times V_{int} \times C_{int\,lipo} \quad (3)$$

Free Dox in tumor cells:

$$V_{tu} \times \frac{dC_{tu}}{dt} = K_{et} \times V_{int} \times C_{int} - K_{te} \times V_{tu} \times C_{tu} \quad (4)$$

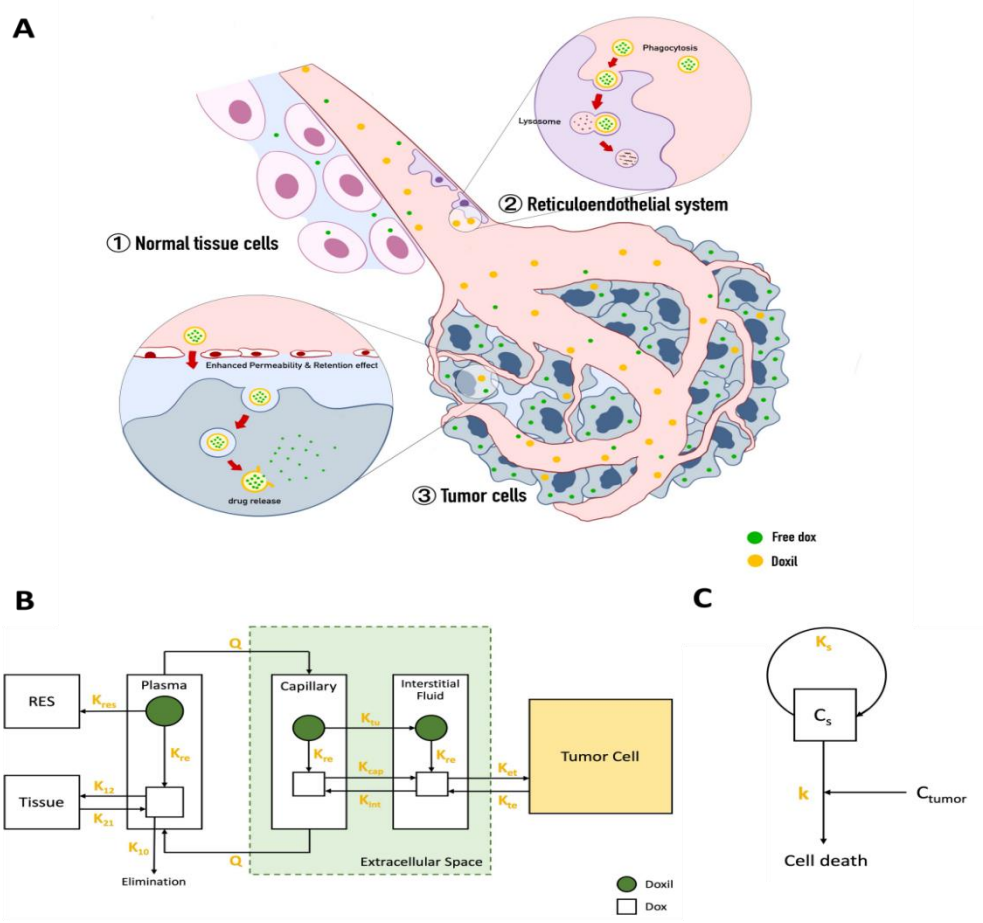

Figure 1. The PK and PD model establishment based on the biological metabolism of Doxil. (A) The biological metabolism of Doxil. (B) The simulated PK model of Doxil in the body. (C) The simulated PD model of Doxil in the body.

Free Dox in plasma:

$$V_p \times \frac{dC_p}{dt} = K_{re} \times V_p \times C_{p\ lipo} - K_{12} \times V_p \times C_p + K_{21} \times V_{ti} \times C_{ti} - K_{10} \times V_p \times C_p + Q \times C_{cap} + Q \times C_p \quad (5)$$

Free Dox in tissue:

$$V_{ti} \times \frac{dC_{ti}}{dt} = K_{12} \times V_p \times C_p - K_{21} \times V_{ti} \times C_{ti} - K_{10} \quad (6)$$

Free Dox in capillary:

$$V_{\text{Cap}} \times \frac{dC_{\text{cap}}}{dt} = K_{re} \times V_{\text{cap}} \times C_{\text{cap lipo}} + K_{\text{int}} \times V_{\text{int}} \times C_{\text{int}} - K_{\text{cap}} \times V_{\text{cap}} \times C_{\text{cap}} - Q \times C_{\text{cap}} \quad (7)$$

Free Dox in interstitial space:

$$\frac{dC_{int}}{dt} = K_{cap} \times V_{cap} \times C_{cap} + K_{re} \times V_{int} \times C_{int\ lipo} + K_{re} \times V_{tu} \times C_{tu} - K_{int} \times V_{int} \times C_{int} - K_{et} \times V_{int} \times C_{int} \quad (8)$$

TABLE I. MODEL PARAMETERS IN PK MODEL

Parameter	Significance	Value
Rate of Doxil transportation between compartments (h-1)		
Kre	Rate of release from Doxil to Dox	0.3/0.03/0.003
Kres	Rate of Doxil uptake by RES	0.5/0.05/0.005
K10	Rate of Doxil elimination	0.56
Ktu	Rate of Doxil transfer from capillary to interstitial space	7.17
Rate of Dox transportation between compartments (h-1)		
K12	Rate of Dox transfer from plasma to tissue	5.13
K21	Rate of Dox transfer from tissue to plasma	0.0927
Kcap	Rate of Dox transfer from capillary to interstitial space	0.527
Kint	Rate of Dox transfer from interstitial to capillary	0.107
Ket	Rate of Dox from extracellular space to tumor cells	2.27
Kte	Rate of tumor cells to extracellular space	0.0485
Volumes of compartments (mL)		
Vcap	Capillary space volume	0.3
Vint	Interstitial space volume	3
Vtu	Tumor space volume	6
Vp	Plasma space volume	500
Rate of blood flow (mL/h/g)		
Q		41.2

TABLE II. VARIABLES

Parameter	Significance	Value
Concentration of drug(μg/mL) **C**tu	Dox concentration in tumor	Change with time
Cint	Dox concentration in interstitial space	Change with time
Cint lipo	Doxil concentration in interstitial space	Change with time
Cp	Dox concentration in plasma	Change with time
Cp lipo	Doxil concentration in tumor	Change with time
Ccap	Dox concentration in capillary	Change with time
Ccap lipo	Doxil concentration in capillary	Change with time
Cti	Dox concentration in tissue	Change with time
Cs	Cell density	Change with time

[13]

B. PD Model

In the PD model (Fig. 1C), we investigated the relationship between drug concentration in the tumor area with drug efficacy. To evaluate the efficacy of Doxil, we introduced a parameter termed cancer cell density C_s. Cell density is affected by two factors: replication of tumor cells and Dox-induced cell deaths. Dox in the active site, which is a portion f_b of the overall Dox concentration in interstitial space C_{int}, causes irreversible tumor cell deaths at a rate k, depending on tumoral sensitivity to Dox. At the same time, tumor cells are proliferating at the rate K_s. Both death and replication are proportional to cell density. This gives the equation of the rate of change of cell density. And parameters are shown in Table III below.

$$\frac{dC_s}{dt} = -k \times f_b \times C_{tu} \times C_s + K_s \times C_s \qquad (9)$$

TABLE III. MODEL PARAMETERS IN PD MODEL

Parameter	Significance	Value
k	Dox-induced irreversible cell death	16.5/10.6/5.4/1.68 /(ug/ml) h-1
fb	Portion of drug in active site	0.2
KS	Proliferation rate	0.171/0.0568/0.0183 h-1

III. RESULT

A. Simulation of Drug Concentration and Antitumor Efficacy by Altering K_{res} and K_{re}

1) Pharmacokinetics

In PK models, we adjusted the release rate of free dox (K_{re}) and the clearance rate of Doxil by RES (K_{res}) to understand the effect of these two factors on PK and PD of Doxil. This study is highly clinically relevant because K_{re} and K_{res} of Doxil are predominantly determined by the chemical compositions, which can be versatilely engineered to achieve optimal efficacy.

The concentration of Dox in the tumor, plasma, capillary, interstitial fluid, and Doxil in Plasma and capillary is shown in Fig. 1. For each row, K_{res} value remains at a set value and K_{re} value varies among 0.3 h^{-1}, 0.03 h^{-1}, and 0.003 h^{-1} to simulate the Doxil PK under different release rate. For each column, K_{re} is constant, whereas the K_{res} value changes among 0.5 h^{-1}, 0.05 h^{-1}, and 0.005 h^{-1}.

In all simulations, liposomal dox concentration has a peak of 100 μg/mL in plasma when the Doxil is intravenously injected, representing the same dose across all the simulations. Then the liposomal dox concentration ($C_{cap\ lipo}$) in the capillary efficiently increases and quickly calibrates with $C_{p\ lipo}$, which is not surprising because Doxil in the capillary is transported by the influx of blood. As Doxil releasing free dox, Doxil concentration in plasma and capillary falls gradually, while free dox diffuses into other compartments, raising concentration.

In the first row, the K_{res} are kept constant at 0.5 h^{-1} and K_{re} varies among 0.3 h^{-1}, 0.03 h^{-1}, and 0.003 h^{-1}, a decreasing K_{re} value (Fig. 2A–2C). The decrease of K_{re} leads to a prolonged half-life of $C_{p\ lipo}$ and $C_{cap\ lipo}$. This indicates that Doxil stability contributes to the circulation lifetime and improves PK. However, the decreased K_{re} causes a slower increase in C_p and C_{int}, which suggests a low concentration of free dox in capillary and plasma. Consequently, the rate of free dox entering the tumor region drops obviously. After 20-hour circulation, K_{re}=0.3 h^{-1} produces a C_{tu} equal to 39.44μg/mL (Fig. 2A). It drops to 21.25μg/mL and 3.196μg/mL in K_{re}=0.03 h^{-1} and 0.003. h^{-1}. In the second row with K_{res}=0.05 h^{-1}, a similar trend is also observed. These results suggested that there is a delicate balance between K_{re} value. A smaller K_{re} value can bring a longer circulation period for the drug, leading to high drug exposure. However, the release of the drug is meanwhile restricted, resulting in low tumor accumulation.

Then we would like to investigate how K_{res} change will affect the PK. When we compare the results within a column, which represents a reduced K_{res}, $C_{p\ lipo}$ and $C_{cap\ lipo}$ show longer half-life, resulting from decreased clearance by RES. Now more Doxil can persist in the body, causing an increased Dox accumulation in the tumor after 20 hours. Quantitatively, K_{res}=0.5 h^{-1} only produces a C_{tu} of 39.44 μg/mL. Decreasing K_{res} to 0.05 raised C_{tu} to 88.93 μg/mL. Further decreasing K_{res} to 0.005 h^{-1} even leads to a C_{tu} as high as 101.4 μg/mL. These results suggest that escaping from RES clearance helps to improve the PK of Doxil, increasing the accumulation of the active drugs in the tumor site.

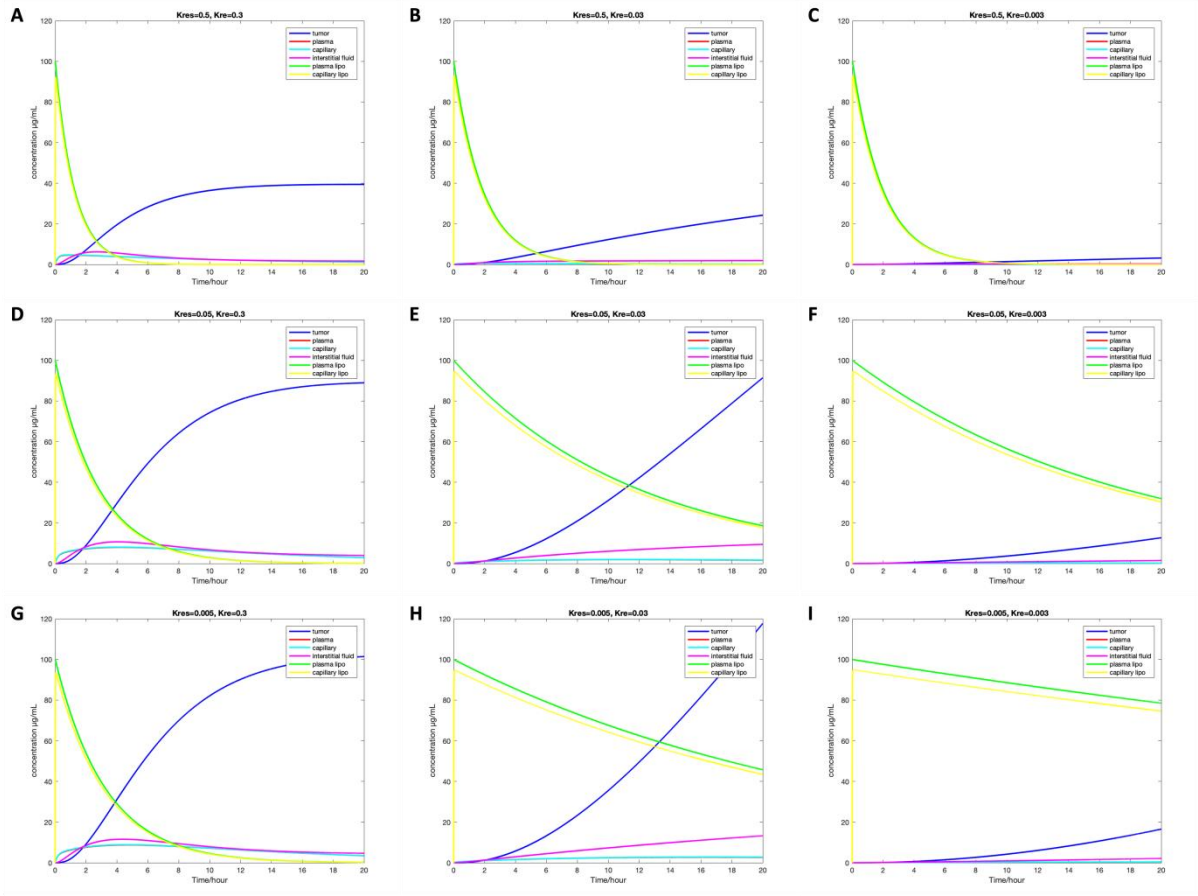

Figure 2. The effect of K_{res} and K_{re} on the PK of Doxil. (A) K_{res}=0.5 h^{-1}, K_{re}=0.3 h^{-1}. (B) K_{res}=0.5 h^{-1}, K_{re}=0.03 h^{-1}. (C) K_{res}=0.5 h^{-1}, K_{re}=0.003 h^{-1}. (D) K_{res}=0.05 h^{-1}, K_{re}=0.3 h^{-1}. (E) K_{res}=0.05 h^{-1}, K_{re}=0.03 h^{-1}. (F) K_{res}=0.05 h^{-1}, K_{re}=0.003 h^{-1}. (G) K_{res}=0.005 h^{-1}, K_{re}=0.3 h^{-1}. (H) K_{res}=0.05 h^{-1}, K_{re}=0.03 h^{-1}. (I) K_{res}=0.005 h^{-1}, K_{re}=0.003 h^{-1}.

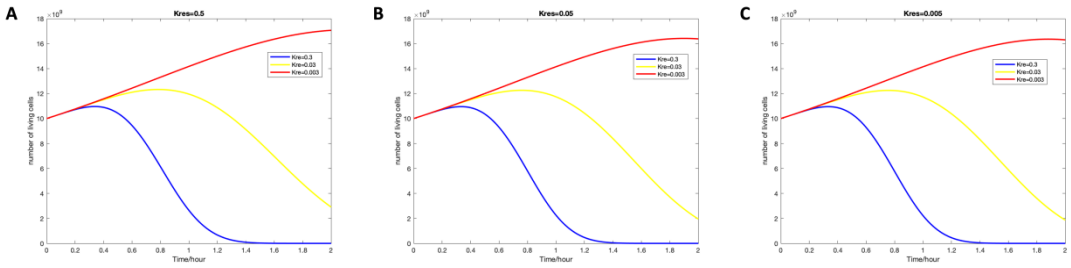

Figure 3. The influence of K_{res} and K_{re} on PD of Doxil.

2) Pharmacodynamics

The antitumor effect is then simulated using cell density C_s. We computed the cell density change in the above K_{res} and K_{re}, as shown in Fig. 3. We found that the line of K_{re}=0.3 h^{-1} quickly eliminates cancer cells while K_{re}=0.03 h^{-1} kills cancer cells at a slower rate. However, when K_{re} is decreased to 0.003 h^{-1}, the tumor growth is out of control, suggesting a weak antitumor effect. After 2 hours in the simulation, the number of living cells with K_{re}=0.003 h^{-1} increases to 5.86 times compared to that of K_{re}=0.03 h^{-1} and 6,010,000 times to that of K_{re}=0.3 h^{-1}.

In view of K_{res}, there is no gigantic difference between the antitumor effect of the drug with K_{res}=0.05 h^{-1} and 0.005 h^{-1}, but they have a slight advantage in contrast to K_{re}=0.5 h^{-1}. Across three graphs, with lines of K_{re}=0.3 h^{-1}, cell number in the tumor region is 3.98% and 4.45% richer in body administrated Doxil with K_{res}=0.5 h^{-1} than K_{res}=0.05 h^{-1} and 0.005 h^{-1} respectively.

B. Simulation of the Effect of Physical Alternation on Antitumor Efficacy

Tumor varies in physical characteristics, such as size and sites, leading to changes in blood influx to the tumor, thereby affecting drug transportation. Those parameters result in different treatment outcomes, which can be caused by the change in PK and PD. Therefore, in this simulation, we modify the flow rate Q to observe any change in PK and PD.

In capillaries, a higher blood flow rate significantly improves Doxil concentration. Without concerning the lymph circulation, a higher blood flow rate allows more Doxil from plasma to enter the capillary by diffusion,

upgrading the Doxil level. In comparison, a lower blood flow rate (9.7 ml/h/g) reaches a lower peak. The second difference can be seen in the tumor's drug concentration level, which is primarily Dox. After 10 hours, flow rate Q=41.2 ml/h/g raised the drug concentration to 36.42 ug/ml, while that of Q=9.7 ml/h/g is only 31.35 ug/ml (Fig. 4A and 4B). It can be concluded that a greater amount of drug is delivered by blood to the tumor.

We then studied the effect of blood flow rates into the tumor (Q) on tumor cell density. In Fig. 4C, the two different tumor blood flow rates (41.2 ml/h/g and 9.7 ml/h/g) resulted in a different number of living cells. A greater amount of dox leads to increased apoptosis of tumor cells, thus decreasing the number of living cells.

As a result, plasma with Q=41.2 ml/h/g has a greater impact on killing tumor cells and reducing the number of living cells, whereas in the case of Q=9.7 ml/h/g, there is only a minor impact on the removal of tumor cells.

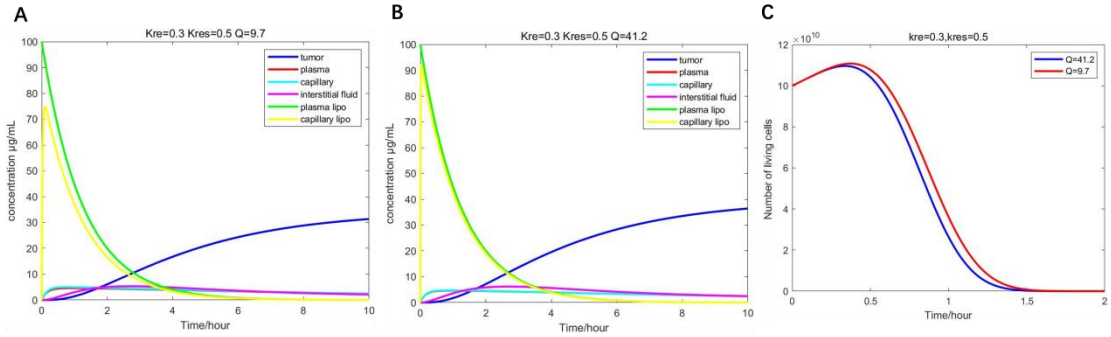

Figure 4. The influence of Q on PD and PK of Doxil. (A) Q=41.2 mL/h/g. (B) Q=9.7 mL/h/g.

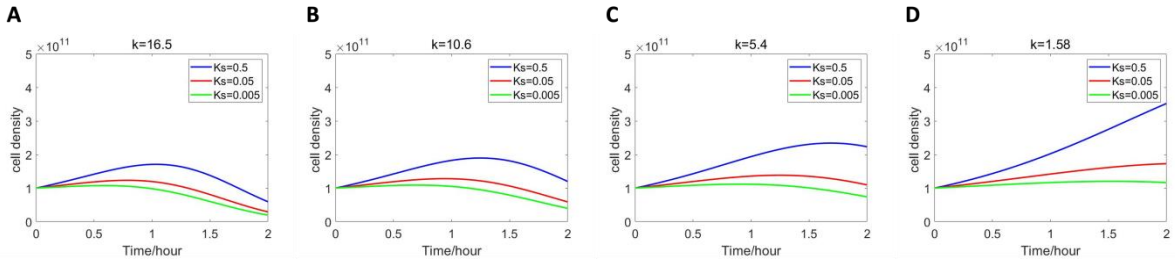

Figure 5. The influence of k and K_s on PD of Doxil. (A) k=15.4 h^{-1}/(ug/ml), K_s=0.724/0.368/0.171 h^{-1}. (B) k=10.6 h^{-1}/(ug/ml), K_s=0.724/0.368/0.171 h^{-1}. (C) k=5.4 h^{-1}/(ug/ml), K_s=0.724/0.368/0.171 h^{-1}. (D) k=1.68 h^{-1}/(ug/ml), K_s=0.724/0.368/0.171 h^{-1}.

C. Simulation of the Effect of Proliferation Rate and Tumor Sensitivity on Antitumor Effect

1) Dox-induced irreversible cell death

The tumor sensitivity to chemotherapy can differ on phenotypes, lineage, and treatment history. Nevertheless, multi-drug resistance is a major limitation of chemotherapy, which is often acquired from long-term exposure to a single drug. Studying tumor sensitivity can provide a rationale to explain how resistance affects treatment outcomes. We adopt multiple values in the model varying from 16.4 h^{-1}/(ug/ml), 10.6 h^{-1}/(ug/ml), 5.4 h^{-1}/(ug/ml), and 1.68 h^{-1}/(ug/ml).

The trend of the antitumor effect decreases when sensitivity to the drug is reduced from 16.4 to 1.68. Taking the lines of K_{re}=0.724 h^{-1} as an example, the rate of cell deaths becomes smaller gradually and remains under 0, as shown in Fig. 5D. Quantitatively evaluating the results at the point of 2 hours, the number of cells remaining in the tumor region is 6.0×10^{10}, 1.2×10^{11}, 2.2×10^{11} and 3.5×10^{11} in each graph, which shows an expeditiously expanding trend.

2) Cell proliferation rate

The replication rate of tumor cells is represented by K_s, a strong indicator of tumor malignancy. It is also an essential factor affecting the antitumor effect, so K_s is altered among the values 0.724 h^{-1}, 0.368 h^{-1}, and 0.171 h^{-1} to compare living cells amount using the PD model. K_s value has an inverse proportion related to the rate of tumor cell deaths. In Fig. 5A–5D, more cells survived when K_s values increased. In Fig. 5D, when tumor cells replicate fast (K_s=0.724 h^{-1}), 3.4×10^{11} cells are left within 2 hours of drug exposure. When the K_s value is lowered to 0.368 h^{-1}, cells remaining are also halved to 1.7×10^{11}. A further diminishment in K_s results in a cell amount of 1.1×10^{11}.

IV. Discussion

Doxil has generally failed to exhibit improved antitumor efficacy compared with free Dox [12]. This has also been demonstrated by our mathematical models, which show a relationship between drug concentration and different K_{re} values. The more extended circulation period and, therefore, a higher drug exposure for drug results from a smaller K_{re} value, suggesting the influence of the stability of the liposomal coat, which controls the bioavailability of Doxorubicin. Meanwhile, although the drug accumulation in the tumor is consequently low, all the other compartments seem to share the same trend (lower drug concentration), leading to lower overall toxicity of Doxil when compared to free Dox. Therefore,

in clinical applications, the best pharmaceutical strategies, including the optimum dosage of Doxil, can be constructed based on the effect of K_{re} on drug exposure and tumor accumulation, where a balance should be set by finding the best distribution between the two factors.

In the same model, the influence of K_{res} on drug concentration is also highlighted, where the cells such as Kupffer cells in the system are considered to play a significant role in clearing liposomes after intravenous administration. As a result, the decrease in the clearing ability of RES can therefore improve the performance of Doxil and increase the active drug accumulation in the tumor.

In the PD model, the relationship between tumor cell proliferation rate and K_{re} and K_{res} has been investigated. We found that a lower value of K_{re} conspicuously points to a weaker antitumor effect, whereas a lower value of K_{res} has led to a general decrease in the number of living cells, whereby less Doxil being cleared by the RES results in higher drug exposure to the tumor cells and therefore kill the cells faster. This may prove the link between high K_{res} and weak proliferation rate. Both results further highlight the effect of K_{re} and K_{res} on the antitumor effect.

Admittedly, compared to other clinical research carried out using actual samples, our computational modeling is limited in complexity, since the complicated composition and functions of real human bodies are almost impossible to simulate comprehensively. Moreover, the physical parameters for each patient can vary, but we use fixed values. Thirdly, our model only applies to solid tumors, which means for 'non-solid cancers' such as leukemias our model does not work. Finally, different physiological barriers are not considered in our model. Particularly, the blood-brain barrier with an intact physiochemical structure to prevent molecule entry is not considered in our model. Hence, this model cannot simulate PK or PD in glioma patients.

Nevertheless, we believe our investigation is valid for the following reasons: (i) although the values we used are fixed, they are the average values calculated from real measurements from the previous research. (ii) The number of compartments seems to be limited, but they are the ones mainly involved in the drug delivery system. These two characteristics both improve the lack of careful consideration in computational modeling to the maximum extent. Then in practical uses, the conclusions and results, including the correlation between drug concentration and K_{res}, drawn from our investigation may well promote further research on effective drug delivery systems and therefore optimize the therapeutic strategies in cancer treatment.

V. Conclusion

We created a physiological model to determine the pharmacokinetics and pharmacodynamics of Doxil, as well as the time course of free Dox in the tumor space, and coupled it to a cell-killing kinetic model to evaluate its anticancer efficacy. To simulate the linkages between intravenously injected Dox and Doxil, the two models in this study use parametric figures of drug transportation in anatomical compartments, including plasma, capillary, interstitial, and tumor cells. By contrasting the pharmacological parameters of Doxil, simulations were carried out to discuss the relationship between the anticancer effect and physicochemical properties. Although our models demonstrate that Doxil has a lower antitumor efficacy than free Dox, this also means that it has a lower toxicity. Potentially, the performance of Doxil and the accumulation of active drug in the tumor could be enhanced by the reduction in RES's clearing capacity. Additionally, we discovered that higher levels of K_{re} and K_{res} may inhibit the proliferation of tumor cells. Consequently, future research could concentrate on these two factors. Given that our research is computation-based, we would encourage future research to do experiments, discover the underlying mechanism, create a more effective drug delivery system, and subsequently better therapeutic options for cancer therapy.

Conflict of Interest

The authors declare no conflict of interest.

Author Contributions

Cherong Ma, Zekai Guo, and Zhiyin Liang conducted the research; Cherong Ma, Zekai Guo, and Zhiyin Liang analyzed the data; Virgia Wang wrote the paper; all authors had approved the final version.

Acknowledgment

We thank our instructors, Dr. Liu and Dr. Alirio Melendez-Romero, for their professional advice and supports throughout this research.

All computational models are constructed and plotted using MATLAB.

References

[1] J. Lakkakula, P. Gujarathi, P. Pansare, *et al.*, "A comprehensive review on alginate-based delivery systems for the delivery of chemotherapeutic agent: Doxorubicin," *Carbohydrate Polymers*, vol. 259, 117696, 2021.

[2] T. Tadokoro, M. Ikeda, T. Ide, *et al.*, "Mitochondria-Dependent ferroptosis plays a pivotal role in doxorubicin cardiotoxicity," *JCI Insight*, vol. 5, no. 9, 2020.

[3] S. Ibsen, E. Zahavy, W. Wrasdilo, *et al.*, "A novel doxorubicin prodrug with controllable photolysis activation for cancer chemotherapy," *Pharm Res.*, vol. 27, pp. 1848–1860, 2010.

[4] S. Sritharan and N. Sivalingam, "A comprehensive review on time-tested anticancer drug doxorubicin," *Life Sciences*, vol. 278, 119527, 2021.

[5] N. N. Zashikhina, M. V. Volokitina, V. A. Korzhikov-Vlakh, *et al.*, "Self-Assembled polypeptide nanoparticles for intracellular irinotecan delivery," *European Journal of Pharmaceutical Sciences*, vol. 109, pp. 1–12, 2017.

[6] K. Gajera and A. Patel, "An overview of FDA approved liposome formulations for cancer therapy," *Journal of Advances in Medical and Pharmaceutical Sciences*, vol. 24, no. 3, pp. 1–7, 2022.

[7] M. Cagel, M. A. Moretton, E. Bernabeu, *et al.*, "Antitumor efficacy and cardiotoxic effect of doxorubicin-loaded mixed micelles in 4T1 murine breast cancer model. Comparative studies using Doxil® and free doxorubicin," *Journal of Drug Delivery Science and Technology*, vol. 56, 101506, 2020.

[8] S. R. Saptarshi, A. Duschl, and A. L. Lopata, "Interaction of nanoparticles with proteins: relation to bio-reactivity of the

nanoparticle," *J. Nanobiotechnology*, vol. 11, article number 26, 2013.
[9] V. H. Nguyen and B. J. Lee, "Protein corona: A new approach for nanomedicine design," *Int. J. Nanomedicine*, vol. 12, pp. 3137–3151, 2017.
[10] M. V. Liberti and J. W. Locasale, "The Warburg effect: How does it benefit cancer cells?" *Trends Biochem. Sci.*, vol. 41, pp. 211–218, 2016.
[11] L. H. Lindner and M. Hossann, "Factors affecting drug release from liposomes," *Curr. Opin. Drug Discov. Devel.*, vol. 13, pp. 111–123, 2010.
[12] D. T. Auguste, K. Furman, A. Wong, *et al.*, "Triggered release of siRNA from poly(ethylene glycol)-protected, pH-dependent liposomes," *J. Control Release*, vol. 130, pp. 266–274, 2008.
[13] Y. Zhao, D. Y. Alakhova, J. O. Kim, *et al.*, "A simple way to enhance Doxil® therapy: Drug release from liposomes at the tumor site by amphiphilic block copolymer," *J. Control Release*, vol. 168, pp. 61–69, 2013.